Theoretical Investigations on the Kinetics of H-Abstraction Reactions from CF3CH(OH)CF3 by OH Radicals

2 AUTHORS:

Srinivasulu Gonu
Indian Institute of Technology Madras
3 PUBLICATIONS   11 CITATIONS

SEE PROFILE

B. Rajakumar
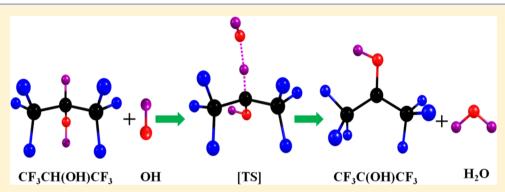Indian Institute of Technology Madras
37 PUBLICATIONS   244 CITATIONS

SEE PROFILE

Theoretical Investigations on the Kinetics of H-Abstraction Reactions from CF$_3$CH(OH)CF$_3$ by OH Radicals

G. Srinivasulu and B. Rajakumar*

Department of Chemistry, Indian Institute of Technology, Madras, Chennai 600036, India

Ⓢ *Supporting Information*

CF$_3$CH(OH)CF$_3$ OH   [TS]   CF$_3$C(OH)CF$_3$ H$_2$O

ABSTRACT: The kinetic studies of the H-abstraction reaction of CF$_3$CH(OH)CF$_3$ with the OH radical, which is predicted to have two classes of possible reaction channels, were carried out. The minimum energy path and energetics were calculated at M062X/6-31+G (d,p) method. The rate coefficients for each reaction channels were evaluated by canonical variational transition state theory (CVT) with the small-curvature tunneling correction (SCT) and zero-curvature tunneling over the wide range of temperature of 200−3000 K. The temperature-dependent rate expression for the title reaction is obtained to be $k_{(Total)} = 2.60 \times 10^{-22} T^{3.04} \exp(372.45/T)$ cm^3 molecule^{-1} s^{-1}; with $k_{(298)} = 3.54 \times 10^{-14}$ cm^3 molecule^{-1} s^{-1}. The global warming potentials (GWPs) and atmospheric lifetimes of CF$_3$CH(OH)CF$_3$ are computed in the present investigation. The atmospheric implications and the degradation mechanism of CF$_3$CH(OH)CF$_3$ are discussed. It is concluded that this compound can be suggested as an acceptable substitute to HFCs in terms of its atmospheric lifetime and GWPs.

1. INTRODUCTION

Fluorinated hydrocarbons (hydrofluorocarbons or HFCs) are the leading ozone-friendly substitutes for chlorofluorocarbons (CFCs).[1] The photochemical ozone creation potential (POCP), a well-established method of ranking compounds by their ability to form ozone in the troposphere,[1] depends on the rate coefficient of the reaction between a compound and OH.[2] Fluorinated alcohols like 2-substituted propanols (for example CF$_3$CH(OH)CF$_3$) are one such class of ozone-friendly chemicals being considered as CFC substitutes as well as in certain industrial applications. CF$_3$CH(OH)CF$_3$ is used as an industrial solvent. Since the CF$_3$CH(OH)CF$_3$ molecule does not contain a chlorine atom, it does not destroy the ozone layer, but it will contribute to global warming. These kind of chemicals are removed from the atmosphere mainly via reaction with the OH radical, which is a significant loss process, also by wet and dry deposition. Hence, OH reaction rate coefficients for such compounds are required to determine their atmospheric lifetimes and possible effects on the Earth's radiation budget (i.e., their GWPs).[3] The fate of the CF$_3$CH(OH)CF$_3$ molecule is expected to be degradation via the reaction with OH radicals. Although an enormous number of investigations on rate coefficients are available in the literature for various alcoholic compounds, very little

information regarding the OH reaction rate coefficients with fluorinated alcohols are available. Two experimental studies were reported on the rate coefficients for the title reaction CF$_3$CH(OH)CF$_3$ + OH → products: One is recently by Orkin et al.[3] where they have measured rate coefficients using a flash photolysis resonance−fluorescence technique over the temperature range of 220−370 K.[3] The other one is by Tokuhashi et al.[4] where the kinetic measurements were carried out using the discharge flow, laser photolysis, and flash photolysis methods, combined respectively with the laser-induced fluorescence technique to monitor the OH radical concentrations over the temperature range of 250−430 K.[4] Atkinson and co-workers have developed a method to predict the OH reaction rate coefficients based on the structure activity relationships (SAR). This method can be applied to various reactions of H-atom abstraction from C−H and O−H bonds, OH addition to double and triple bonds, and so forth. However, they have noticed and reported that the SAR method does not work well for the compounds such as CHF$_3$, CH$_3$CF$_3$, CHF$_2$CF$_2$CF$_2$CF$_2$H, and fluorinated ethers. Tokuhashi et al.[4]

reexamined the prediction method for the H-abstraction rate coefficients from C−H and O−H bonds, and the total reaction rate coefficient for the H-abstraction is obtained as the sum of contributions from each C−H and O−H bond present in the molecule. The estimated and experimental rate coefficients of $CF_3CH(OH)CF_3$ with OH at 298 K reported by Tokuhashi et al.
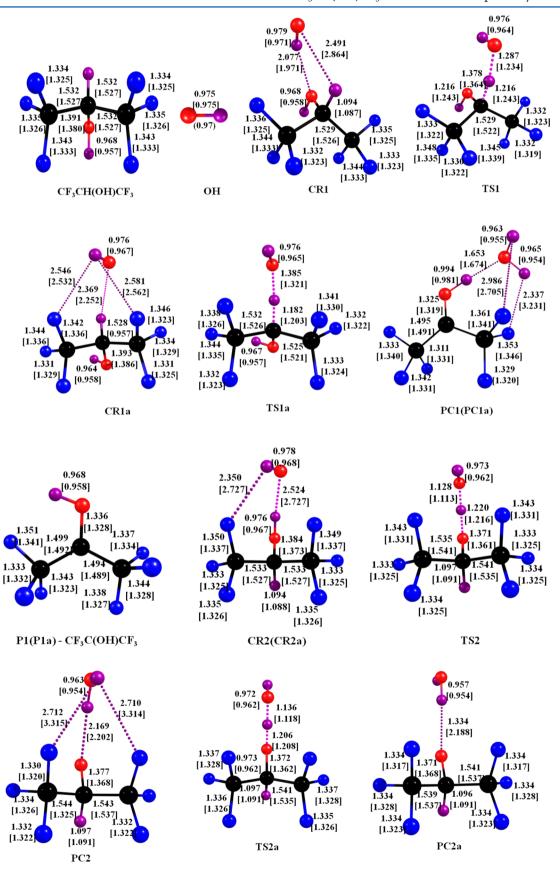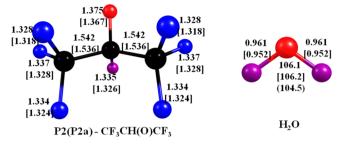

Figure 1. continued

Figure 1. Optimized geometries of reactants, reaction complexes, transition states, and products obtained at M06-2X/6-31+G(d, p), MPW1K/6-31+G(d,p) (in square brackets), and experimental values (in parentheses). Bond lengths are in angstroms, and angles are in degrees. Black represents carbon, blue represents fluorine, red represents oxygen, purple color represents hydrogen, and purple color dotted lines represents hydrogen bond formation.

are 2.51×10^{-14} and 2.52×10^{-14} cm^3 molecule^{-1} s^{-1}, respectively. The rate coefficient determined by Orkin et al. is $(2.49 \pm 0.06) \times 10^{-14}$ cm^3 molecule^{-1} s^{-1} at 298 K.

Although two experimentally measured rate coefficients are available on the title reaction, no theoretical studies were reported so far to the best of our knowledge. The aim of this present study is to provide a deep insight into the reaction of the $CF_3CH(OH)CF_3$ with OH radicals. Both Orkin and Tokuhashi's groups have covered the temperature range of 220−370 K and 250−430 K, respectively. In our investigations, we have explored the kinetics in the temperature range of 200−3000 K, which will be of use in all practical purposes like modeling of both atmospheric and combustion kinetics. The rate coefficients for the title reaction are calculated by canonical variational transition state theory (CVT)[5−7] in the temperature range of 200−3000 K. The small-curvature tunneling (SCT)[8,9] correction is included. The comparisons between theoretical and experimental results are discussed, and also the atmospheric degradation mechanism and atmospheric implications of $CF_3CH(OH)CF_3$ are discussed.

2. COMPUTATIONAL METHODS

The geometries and harmonic vibrational frequencies of all stationary points (the reactants $CF_3CH(OH)CF_3$, OH, transition states (TSs), products, and reaction complexes (RCs)) for the abstraction of the hydrogen atom reactions were optimized at the M06-2X[10,11] level of theory with the 6-31+G(d,p) basis set. In addition to this, to validate the accuracy of the structure and energies of the stationary points, calculations are also carried out using a modified Perdew−Wang one parameter method (MPW1K)[12] with the 6-31+G(d,p) basis set. The M06-2X method, which was developed for main-group thermochemistry and kinetics calculations, has shown to be more accurate than previously introduced MPW1K and MPWB1K methods.[12,13] The M06-2X/6-31+G(d,p) method was reported to be sufficiently accurate for predicting reliable geometries and frequencies of the stationary points, in earlier studies.[14−18] The minimum energy path (MEP)[19] was constructed with intrinsic reaction coordinate (IRC)[20] calculations using M06-2X/6-31+G(d,p) to verify that the transition states connect the designated local minima.

All of the electronic structure calculations were carried out using the Gaussian 09 program suite.[21] The normal mode vibrational frequencies of reactants, intermediates, transition states, and products are viewed in Gauss View.[22] On the basis of this primary information (optimized geometries, energies, and frequencies along the MEP), the kinetic calculations for title reaction were carried out by canonical variational transition

state theory (CVT)[5−7] using POLYRATE 2008 program[23] and GAUSSRATE 2009A.[24] The theoretical rate coefficients for title reaction over the wide temperature range of 200−3000 K are calculated using CVT including the small-curvature tunneling correction (SCT)[8,9] method proposed by Truhlar and co-workers. The thermal rate coefficients of CVT, $k^{CVT}(T)$, are formulated as follows.

$$k^{CVT}(T) = \min k^{GT}(T, s) = k^{GT}(T, s^{CVT}(T)) \qquad (1)$$

where s is a reaction coordinate parameter that determines location of the generalized dividing surface, $s^{CVT}(T)$ is a specific value of s at which the canonical variational transition state rate coefficient is calculated. $k^{GT}(T, s)$ is the generalized transition state rate coefficient that is evaluated at the dividing surface and is expressed as follows:

$$k^{GT}(T, s) = \sigma \frac{k_B T}{h}\left(\frac{Q^{GT}(T, s)}{\Phi^R(T)}\right)\exp\left(\frac{-V_{MEP}(s)}{k_B T}\right) \qquad (2)$$

Here, $V_{MEP}(s)$ is the classical potential energy of generalized transition state at s. Q^{GT} is the canonical partition function of the generalized transition state at s, Φ^R is the reactant's partition function per unit volume, h is Planck's constant, σ is reaction path degeneracy, k_B is Boltzmann's constant, and T is temperature in Kelvin. In the calculations of electronic partition function, the ground state $^2\Pi$ of OH radical, with a 140 cm^{-1} splitting, is taken into account.[25]

3. RESULTS AND DISCUSSION

3.1. Electronic Structures of Stationary Points. Optimized geometric parameters of the reactants, transition states (TS's), products, and hydrogen-bonded complexes (HBCs) at M06-2X/6-31+g(d,p) theory are shown in Figure 1, along with the available experimental values of H_2O and OH.[26] The reactants, TS's, products, and hydrogen-bonded complexes (cf Figure 1: CR1, CR1a, CR2, CR2a, PC1, PC1a, and PC2) are also calculated at MPW1K/6-31+G(d,p) level of theory, and corresponding results are shown in the same figure for comparison. As shown in Figure 1 the optimized geometrical parameters obtained at the two level of theories are reasonably in good agreement with each other. The structural parameters are given in Table S-I of the Supporting Information. In this study we have observed two classes of reaction channels for this title reaction: One is hydrogen abstraction from the methyne (−CH−) position, represented by R1, and the second one is hydrogen abstraction from the hydroxyl (−OH) position, represented by R2, as follows:
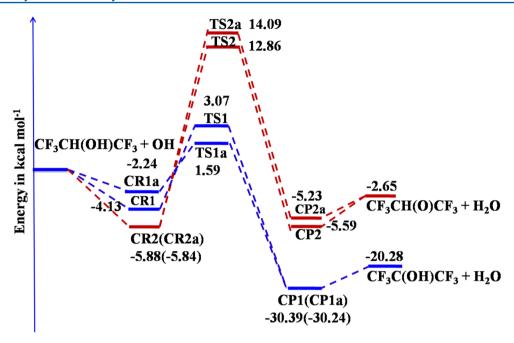
Figure 2. Schematic potential energy surface for the CF$_3$CH(OH)CF$_3$ + OH reaction through all four transition states corresponding to reaction channels R1 (TS1, TS1a) and R2 (TS2, TS2a) obtained at the M06-2X/6-31+G(d,p) level of theory.

$$CF_3CH(OH)CF_3 + OH \rightarrow CF_3C(OH)CF_3 + H_2O \quad (R1)$$

$$CF_3CH(OH)CF_3 + OH \rightarrow CF_3CH(O)CF_3 + H_2O \quad (R2)$$

For the reaction channels R1 and R2, total four transition states, namely, TS1, TS1a, TS2, and TS2a, were located (However, only two transition states, namely, TS1a and TS2, are considered in our calculations, as they follow the minimum energy path, vide infra) . In the case of TS1 and TS1a, the length of the breaking C–H bond is elongated by 10% and 8%, with respect to the C–H equilibrium bond length in CF$_3$CH(OH)CF$_3$, and the newly forming H–O bond is longer than the H–O equilibrium bond length in isolated H$_2$O by 25% and 31%, respectively. In the case of TS2 and TS2a, the breaking O–H bond is elongated by 25% and 19%, and the forming H–O bond is stretched by 15% and 15%, respectively, in comparison to the regular H–O bond length in water. The elongation of the breaking bond in case of TS1 and TS1a (C–H or O–H) is less than that of the forming bond (H–O), indicating that these two transition states are reactant-like; that is, the reaction may proceed via an "early" transition state as expected for the exothermic reaction, whereas in the case of TS2 and TS2a, the elongation of the breaking bond (O–H) is slightly more than that of the forming bond (H–O), indicating that the reaction may proceed via a "late" transition state as indicated in Figure 1. In addition, due to electro negativity of the oxygen and fluorine atoms, hydrogen bonds are formed between O and H atoms as well as F and H atoms. So, the hydrogen-bonded complexes with energies less than the reactants or products are located at the entrance and exit channels, respectively. In the hydrogen-bonded complexes the hydrogen bond lengths of O···H and H···F are less than the sum of their van der Waals radii (2.72 and 2.67 Å), for example in the complex CR1a, the bond lengths of O···H and H···F are 2.37 Å and 2.54 Å, respectively, less than the sum of their van der Waals radii, which are 2.72 Å and 2.67 Å, respectively.

The vibrational frequencies of the stationary points were calculated and are given in Table S-II of Supporting Information. The number of imaginary frequencies (zero or one) indicates whether a minimum or transition state has been identified. All of the optimized geometries of the reactants, complexes, and products were confirmed with zero imaginary frequency (NImag = 0), and TS's were confirmed with one imaginary frequency (NImag = 1), the values of imaginary frequencies calculated for TS1, TS1a, TS2, and TS2a at the M06-2X/6-31+G(d,p) theory are 1504i, 973i, 3307i, and 3314i cm^{-1}, respectively.

3.2. Energetics. A schematic potential energy surface of the title reaction obtained at the M06-2X/6-31+G(d,p) level of theory with zero point energy (ZPE) corrections is plotted in Figure 2. The energy of the reactant is set to zero for reference. For reaction channels R1 and R2, the hydrogen bonded complexes (CR1, CR1a, CR2, and CR2a) are located by the hydrogen-bond attractive interaction between O and H and between F and H (as shown in Figure 1), due to the high electro negativities of fluorine and oxygen atoms. At entrance of reaction channel, the energies of CR1, CR1a, CR2, and CR2a are lower than those of the reactants by 4.13, 2.24, 5.88, and 5.84 kcal/mol, respectively, at M06-2X theory. We identified that CR2 and CR2a are energetically and structurally same. On the other hand at the exit of the reaction channels, the energies of product complexes CP1, CP1a, CP2, and CP2a are lower than those of products by 10.11, 9.96, 2.94, and 2.57 kcal/mol, respectively. We have noticed that, in reaction R1, two product complexes CP1 and CP1a are approximately similar structurally and energetically; and they are located with relative energy of 9.96 kcal/mol, less than the corresponding products CF$_3$C(OH)CF$_3$ + H$_2$O. Also, these product complexes are stabilized by the hydrogen bonding between O and H and between F and H. From Figure 1 it is clear that a prereactive complex RC1a is influenced by the interaction between the H atom in the OH radical and the F atoms in the HFIP, and they are 2.5 Å apart, which represents a hydrogen bond interaction and is responsible for the stabilization. In the case of TS1 and TS1a, the potential barriers with ZPE corrections are 3.07 and 1.59 kcal/mol for H-abstraction from the –CH–

Table 1. Relative Energies and Enthalpies (in kcal/mol) Calculated at Various Level of Theories

| | | ΔE | | | ΔH^0_{298} | |
| | R1 | | R2 | | | |
method	TS1	TS1a	TS2	TS2a	R1	R2
M06-2X/6-31+G(d,p)	3.07	1.59	12.86	14.09	−19.89	−2.57
MPW1K/6-31+G(d,p)	5.37	3.52	17.04	17.90	−19.02	−2.73

Table 2. BSSE Corrected Binding Energies (kcal/mol) of Hydrogen-Bonded Complexes and Transition States at M062X and MPW1K Level of Theories

| | M06-2X/6-31+G(d,p) | | | MPW1K/6-31+G(d,p) | | |
compound	without BSSE corrections	BSSE	BSSE and ZPE corrected	without BSSE corrections	BSSE	BSSE and ZPE corrected
CR1a	−2.24	0.65	−1.6	−2.95	0.77	−2.18
CR2	−5.88	0.86	−5.03	−4.47	0.78	−3.69
TS1a	1.59	0.13	1.72	3.52	1.05	4.58
TS2	12.86	0.17	13.03	17.04	1.14	18.18
CP1a	−30.2	2.93	−27.30	−27.74	2.31	−25.43
CP2	−5.59	1.00	−4.59	−3.13	0.89	−2.23

position at M06-2X/6-31+G(d,p) theory. The potential barrier height of TS1a is about 1.58 kcal/mol lower than that of TS1, and both pathways lead to same product $CF_3C(OH)CF_3$ as shown in Figure 2. In the case of R2, the hydrogen abstraction from the −OH− position involve barrier heights of 12.86 and 14.09 kcal/mol with respect to the reactants at M06-2X/6-31+G(d,p) theory, which is higher than those of TS1 and TS1a by 9.79 and 2.50 kcal/mol, respectively. Therefore, as can be seen from Table 1, R2 is less exothermic than R1 by about 17.32 kcal/mol. Therefore, reaction R2 may be thermodynamically less favorable than R1; that is, the title reaction will proceed mainly through the channel of H- abstraction from the −CH− group, while the hydrogen abstraction from the −OH− group is a minor channel. To prove further which one is favorable reaction channel, we estimated the bond dissociation energies (BDEs) of the breaking C−H bond and O−H bond at M06-2X/6-31+g(d,p) theory. The bond dissociation energy of the O−H bond (107.14 kcal/mol) is higher than that of the C−H bond (89.70 kcal/mol) by about 17 kcal/mol; it suggests that H-abstraction from the −CH− position should predominate the reaction. This conclusion can be further verified by rate coefficient data in the following section. The corresponding barrier heights obtained at M06-2X/6-31+G(d,p) theory are given in Table 1.

The dispersion interactions play a major role in stabilizing hydrogen bonded complexes (HBCs) and TS structures. To explain the stability of HBCs and TS's we have computed the basis-set superposition error (BSSE) corrected binding energies for TS's and HBCs using the counterpoise method (CP).[27] Binding energies were estimated from the following equation.

$$\Delta E = \Delta E_{\text{Complexes or TS}} - E_{\text{Reactant1}} - E_{\text{Reactant2}}$$

where $E_{\text{Complexes or TS}}$ is the energy of the hydrogen bonded-complexes or transition states, $E_{\text{Reactant1}}$ is the energy of the most stable $CF_3CH(OH)CF_3$ structure, and $E_{\text{Reactant2}}$ is the energy of the hydroxyl radical. The calculated binding energies of reaction complexes, product complexes and transition states at M062X and MPW1K level of theories are given in Table 2. It is obvious from Table 2 that, the product complex CP1a is more stable (−27.3 kcal/mol and −25.43 kcal/mol) than the

reaction complex CR1a (−1.6 and −2.18 kcal/mol), whereas CP2 is less stable (−4.59 and −2.23 kcal/mol) than the reaction complex CR2 (−5.03 and −3.69 kcal/mol). Transition state TS1a is more stable (1.72 and 4.58 kcal/mol) than the TS2 (13.03 and 18.18 kcal/mol). (The values given in the parentheses are the binding energies obtained at M062X and MPW1K theories, respectively).

The calculated reaction enthalpies $\Delta H^0_{r,298}$ of two reaction channels at both the theories are listed in Table 1. It is found that all reactions are exothermic in nature. The reaction enthalpies of −19.89 and −2.87 kcal/mol for R1 and R2, respectively, obtained at M06-2X/6-31+G(d,p) level of theory, which are in good agreement with the results obtained at MPW1K/6-31+g(d,p) theory (−19.02 kcal/mol for R1 and −2.73 kcal/mol for R2). The largest deviation between these two methods is only 0.8 kcal/mol.

3.3. Reaction Path Properties. The kinetic calculations were performed for the H-abstraction reactions R1 and R2 using the optimized structures and energies obtained in this study. The minimum-energy paths (MEPs) of reactions R1 and R2 are computed by the intrinsic reaction coordinate (IRC) calculations at M06-2X/6-31+G(d,p) theory. Figure 3 shows the plots of the classical potential energy, V_{MEP}, the vibrational ground-state adiabatic potential energy, V_a^G, and the zero-point energy (ZPE) for R1 (TS1a) as functions of the intrinsic coordinate s (amu)$^{1/2}$bohr at M06-2X/6-31+G(d,p) level of theory, where $V_a^G = V_{\text{MEP}} + \text{ZPE}$. Based on results, we have noticed that in the reaction channel R1, TS1, and TS1a have similar characteristics. However, TS1a follows the MEP, and therefore, this TS alone was used in the rate coefficient calculations. Therefore, here we discuss reaction channel going through TS1a in this section. From Figure 3, V_{MEP} and V_a^G curves are similar in shape, and the maximum values of V_{MEP} and V_a^G are located approximately at the same position on the reaction path, that is, at $s = 0$. The ZPE, which is difference between V_a^G and V_{MEP}, shows a little change near the saddle point, with the reaction coordinate s varies. This is also an evidence to show that for the title reaction the variation effect is small or almost negligible. The existence of a small variational effect has been frequently reported in a number of previous articles for H-abstraction reactions.[28−34]
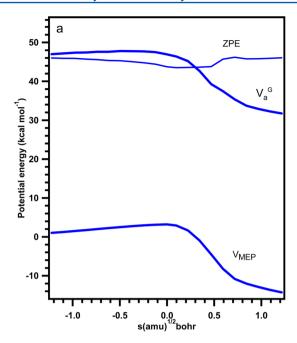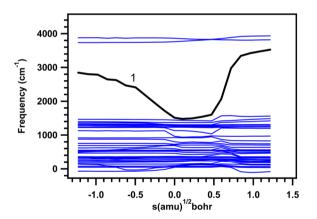
Figure 3. Plots of classical potential energy curve (V_{MEP}), ground-state vibrationally adiabatic energy curve (V_a^G), and zero-point energy curve (ZPE) as functions of s (amu) bohr at the M062X-6-31+G(d,p) level (a) for reaction channel R1(TS1a), $CF_3CH(OH)CF_3 + OH \rightarrow CF_3C(OH)CF_3 + H_2O$.

Figure 4. Changes of the generalized normal mode vibrational frequencies as function of s (amu)$^{1/2}$ bohr at M06-2X/6-31+G(d,p) theory, for reaction R1(TS1a).

Figure 4 shows the variations of the generalized normal-mode vibrational frequencies along the MEPs of reaction R1, that is, TS1a. In Figure 4 the frequencies at about $s = -1.0$ (amu)$^{1/2}$ bohr in the reactant region are associated with those of reaction complex; on the other hand in the product region at about $s = 1.0$ (amu)$^{1/2}$ bohr, the frequencies are associated with those of product complex. While the reaction proceeds, most of those frequencies do not change significantly on going from the reactants to the products, except the frequency mode of 1, shown as the solid black line in Figure 4 called the "reactive mode", and its frequency changes dramatically near the saddle point. This kind of mode is typical character for hydrogen transfer reactions.

3.4. Rate Coefficient Calculations. As mentioned earlier, it should be noted here that, the transition states TS1a and TS2 follow the minimum energy path (MEP). Therefore, only the

minimum energy transition states TS1a and TS2 were taken into account in our rate coefficient calculations. The rate coefficients for the H-abstraction reactions of $CF_3CH(OH)CF_3 + OH$ are computed by using transition state theory (TST), canonical variational transition state theory (CVT), and CVT with small curvature tunnelling (SCT) correction method over the temperature range of 200−3000 K. The rate coefficient of the reaction channel R1 (H-abstraction from the −CH− position) is the rate coefficient of the reaction going through the transition state TS1a and is denoted by k_{R1}; and that of the reaction channel R2 (H-abstraction from OH position) is the rate coefficient of the reaction going through the transition state TS2 and is denoted by k_{R2}. The total rate coefficient ($k^{CVT/SCT}$) is obtained by the summation of the individual rate coefficients of two reaction channels R1 and R2 ($k = k_{R1} + k_{R2}$), and they are given in Table 3. The CVT/SCT rate coefficients computed in the present study along with the corresponding experimental ones are given in Table 3 and plotted in Figure 5.

From Table 3, it can be seen clearly that the rate coefficients obtained using CVT/SCT are greater than those obtained using CVT/ZCT values at lower temperatures; however, at higher temperatures, the rate coefficients are closer to each other. For example, at 200 K, the CVT/SCT rate coefficient is 1.34×10^{-14} cm^3 molecule^{-1} s^{-1}, whereas the CVT/ZCT rate coefficient is 1.10×10^{-14} cm^3 molecule^{-1} s^{-1}. At 3000 K the rate coefficients computed by both methods CVT/SCT and CVT/ZCT are equal which is 1.26×10^{-14} cm^3 molecule^{-1} s^{-1}. We noticed that the CVT/ZCT and CVT/SCT rate coefficients are in better agreement with the available experimental values.[3,4] The computed rate coefficients for the title reactions are plotted in Figure 5. The data were fit to an Arrhenius equation using a three-parameter fit, in the studied temperature range of 200−3000 K. The rate expression for the title reaction is obtained to be $k_{(Total)} = 2.60 \times 10^{-22}\ T^{3.04}$ exp(372.45/T) cm^3 molecule^{-1} s^{-1}.

The rate coefficients for the reaction through channel R1 (through TS1a) were computed using TST and CVT and are tabulated in Table 4. The TST and CVT rate coefficients are nearly the same over the whole temperature range 200−3000 K, and also the variational effect (k^{TST}/k^{CVT}) for this channel (R1) of the reaction varies from 0.61 to 0.51 with temperature. This effect is less than unity over the whole temperature range, which suggests that the variational effect on the rate coefficient is very small or almost negligible for reaction going through channel R1 (through TS1a).

The temperature dependence of the $K_{R1}/k_{(total)}$ and $k_{R2}/k_{(total)}$ branching ratios are plotted in Figure 6. It is clear from Figure 6 that, for the title reaction, channel R1 plays a more important role toward total reaction (hydrogen abstractions from the −CH− group), and the contribution from channel R2 (H-abstraction from the −OH− group) can be neglected over the whole temperature range 200−3000 K. The percentage contributions of k_{R1} and k_{R2} to the total rate coefficient values for the title reaction, over the temperature range of 200−3000 K are given in Table 5. It is clear from this table that the contribution of reaction channel R2 is negligible in the studied temperature range.
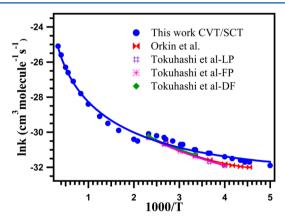
4. ATMOSPHERIC IMPLICATIONS

4.1. Atmospheric Lifetime. The atmospheric lifetime of alcohols released into the atmosphere mainly depends on the rates of several processes via reaction with free radicals like OH,

Table 3. Calculated Rate Coefficients (in cm^3 molecule^{-1} s^{-1}) for the Reaction CF$_3$CH(OH)CF$_3$ + OH → Products in the Temperature Range of 200−3000 K at the M06-2X/6-31+G(d,p) Theory

T (K)	R1(TS1a) CVT/SCT	R2(TS2) CVT/SCT	total CVT/SCT	total CVT/ZCT	exptl values at 298 K
200	1.34×10^{-14}	1.14×10^{-21}	1.34×10^{-14}	1.10×10^{-14}	$^a 2.49 \times 10^{-14}$
220	1.66×10^{-14}	1.28×10^{-21}	1.66×10^{-14}	1.39×10^{-14}	$^b 2.58 \times 10^{-14}$ DF-LIF
225	1.75×10^{-14}	1.33×10^{-21}	1.75×10^{-14}	1.48×10^{-14}	$^b 2.65 \times 10^{-14}$ LP-LIF
230	1.84×10^{-14}	1.38×10^{-21}	1.84×10^{-14}	1.56×10^{-14}	$^b 2.34 \times 10^{-14}$ FP-LIF
240	2.04×10^{-14}	1.48×10^{-21}	2.04×10^{-14}	1.75×10^{-14}	
250	2.25×10^{-14}	1.61×10^{-21}	2.25×10^{-14}	1.95×10^{-14}	
272	2.79×10^{-14}	1.99×10^{-21}	2.79×10^{-14}	2.46×10^{-14}	
275	2.87×10^{-14}	2.05×10^{-21}	2.87×10^{-14}	2.54×10^{-14}	
298^c	$\mathbf{3.54 \times 10^{-14}}$	$\mathbf{2.69 \times 10^{-21}}$	$\mathbf{3.54 \times 10^{-14}}$	$\mathbf{3.19 \times 10^{-14}}$	
300	3.61×10^{-14}	2.75×10^{-21}	3.61×10^{-14}	3.25×10^{-14}	
325	4.48×10^{-14}	3.88×10^{-21}	4.48×10^{-14}	4.09×10^{-14}	
330	4.67×10^{-14}	4.17×10^{-21}	4.67×10^{-14}	4.27×10^{-14}	
350	5.49×10^{-14}	5.66×10^{-21}	5.49×10^{-14}	5.07×10^{-14}	
370	6.42×10^{-14}	7.80×10^{-21}	6.42×10^{-14}	5.98×10^{-14}	
375	6.67×10^{-14}	8.46×10^{-21}	6.67×10^{-14}	6.22×10^{-14}	
400	7.46×10^{-14}	1.28×10^{-20}	7.46×10^{-14}	7.01×10^{-14}	
430	8.82×10^{-14}	2.08×10^{-20}	8.82×10^{-14}	8.36×10^{-14}	
480	5.59×10^{-14}	4.51×10^{-20}	5.59×10^{-14}	5.35×10^{-14}	
500	6.35×10^{-14}	6.05×10^{-20}	6.35×10^{-14}	6.10×10^{-14}	
600	9.88×10^{-14}	2.25×10^{-19}	9.88×10^{-14}	9.60×10^{-14}	
700	1.59×10^{-13}	6.71×10^{-19}	1.59×10^{-13}	1.56×10^{-13}	
800	2.41×10^{-13}	1.69×10^{-18}	2.41×10^{-13}	2.37×10^{-13}	
1000	4.82×10^{-13}	7.40×10^{-18}	4.82×10^{-13}	4.77×10^{-13}	
1200	8.47×10^{-13}	2.34×10^{-17}	8.47×10^{-13}	8.41×10^{-13}	
1500	1.67×10^{-12}	8.83×10^{-17}	1.67×10^{-12}	1.66×10^{-12}	
1800	2.88×10^{-12}	1.05×10^{-15}	2.88×10^{-12}	2.87×10^{-12}	
2000	3.92×10^{-12}	1.83×10^{-15}	3.92×10^{-12}	3.91×10^{-12}	
2500	7.50×10^{-12}	5.62×10^{-15}	7.51×10^{-12}	7.50×10^{-12}	
3000	1.26×10^{-11}	1.32×10^{-14}	1.26×10^{-11}	1.26×10^{-11}	

^{a}Orkin et al.[3] ^{b}Tokuhashi et al.[4] ^{c}The rate coefficient of the title reaction at 298 K is given in **bold** font.

Figure 5. Arrhenius plot of CVT/SCT rate constants calculated at the M06-2X/6-31+G(d,p) theory between 200 and 3000 K for the CF$_3$CH(OH)CF$_3$ + OH reaction.

Cl, and NO$_3$. Among these species, the reactions with the hydroxyl radical in the atmosphere plays a major role in determining the compound's lifetime, as it is considered to be the detergent of the atmosphere and most powerful oxidizing agent. The atmospheric lifetime of hexafluoroisopropanol due to its reaction with tropospheric hydroxyl radicals was estimated by the following equation.

$$\tau_{OH} = \frac{1}{k_{OH}[OH]}$$

where k_{OH} is the rate coefficient of the title reaction at 272 K. The atmospheric lifetime of hexafluoroisopropanol (HFIP) is computed to be 1.2 years, which is a long lifetime. This is reasonably in good agreement with the reported value (1.9 years). However, in the recent studies by Orkin et al.[3] highlighted that these lifetimes can be further shortened if wet deposition plays a significant role in the atmospheric removal of these compounds.
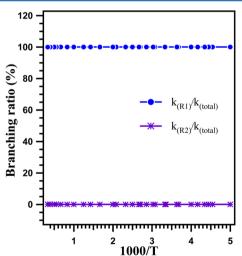
4.2. Global Warming Potentials (GWPs). The global warming potentials[35,36] of hexafluoroisopropanol (HFIP) were estimated using time-integrated radiative forcing of the specific gas, relative to a reference gas such as carbon dioxide[37,38] by combining their radiative forcing, atmospheric lifetime of the gas, and radiative forcing of the reference gas (CO$_2$). The scaled vibrational frequencies (v_k),[39] intensities (A_k) of the corresponding vibrational mode k, and lifetime (τ) are obtained by M06-2X/6-31+G(d,p) theory. In the present test molecule (CF$_3$CH(OH)CF$_3$), because of the absence of either the Cl or Br atom, it will have a negligible ozone depletion potential (ODP). So, our interest is to determine the GWP of CF$_3$CH(OH)CF$_3$.

$$GWP = \frac{a \int_{TH}^{0} e^{-t/\tau} dt}{AGWP_{CO_2}}$$

$$a = \sum_k A_k F(v_k)$$

4540

dx.doi.org/10.1021/jp4006907 | J. Phys. Chem. A 2013, 117, 4534−4544

Table 4. Calculated Rate Coefficients (in cm^3 molecule^{-1} s^{-1}) using TST and CVT for the Reaction CF$_3$CH(OH)CF$_3$ + OH → CF$_3$C(OH)CF$_3$ + H$_2$O (Channel R1(TS1a))

T (K)	TST	CVT
200	2.77×10^{-14}	1.69×10^{-14}
220	3.46×10^{-14}	2.26×10^{-14}
225	3.64×10^{-14}	2.42×10^{-14}
230	3.83×10^{-14}	2.58×10^{-14}
240	4.22×10^{-14}	2.92×10^{-14}
250	4.64×10^{-14}	3.29×10^{-14}
272	5.62×10^{-14}	4.18×10^{-14}
275	5.76×10^{-14}	4.31×10^{-14}
298	6.92×10^{-14}	5.40×10^{-14}
300	7.03×10^{-14}	5.50×10^{-14}
325	8.44×10^{-14}	6.87×10^{-14}
330	8.75×10^{-14}	7.17×10^{-14}
350	1.00×10^{-13}	8.43×10^{-14}
370	1.14×10^{-13}	9.83×10^{-14}
375	1.18×10^{-13}	1.02×10^{-13}
400	1.37×10^{-13}	1.16×10^{-13}
430	1.63×10^{-13}	1.37×10^{-13}
480	2.13×10^{-13}	2.05×10^{-13}
500	2.35×10^{-13}	2.22×10^{-13}
600	3.74×10^{-13}	2.93×10^{-13}
700	5.60×10^{-13}	4.15×10^{-13}
800	8.04×10^{-13}	5.69×10^{-13}
1000	1.50×10^{-12}	9.93×10^{-13}
1200	2.52×10^{-12}	1.59×10^{-12}
1500	4.82×10^{-12}	2.88×10^{-12}
1800	8.21×10^{-12}	4.70×10^{-12}
2000	1.12×10^{-11}	6.24×10^{-12}
2500	2.13×10^{-11}	1.14×10^{-11}
3000	3.60×10^{-11}	1.84×10^{-11}

Table 5. Percentage Contribution of Individual Rate Coefficients k_{R1} and k_{R2} to the Total Rate Coefficient for the Reaction of OH with CF$_3$CH(OH)CF$_3$ over the Temperature Range of 200−3000 K

T (K)	percentage contribution to k_{Total}	
	K_{R1}	K_{R2}
200	100	8.51×10^{-6}
220	100	7.71×10^{-8}
225	100	7.60×10^{-8}
230	100	7.50×10^{-8}
240	100	7.25×10^{-8}
250	100	7.16×10^{-8}
272	100	7.13×10^{-8}
275	100	7.14×10^{-8}
298	100	7.60×10^{-8}
300	100	7.62×10^{-8}
325	100	8.66×10^{-8}
330	100	8.93×10^{-8}
350	100	1.03×10^{-7}
370	100	1.21×10^{-7}
375	100	1.27×10^{-7}
400	100	1.72×10^{-7}
430	100	2.36×10^{-7}
480	100	8.07×10^{-7}
500	100	9.53×10^{-7}
600	100	2.28×10^{-6}
700	100	4.22×10^{-6}
800	100	7.01×10^{-6}
1000	100	1.54×10^{-5}
1200	100	2.76×10^{-5}
1500	99.99	5.29×10^{-5}
1800	99.96	3.64×10^{-4}
2000	99.95	4.67×10^{-4}
2500	99.93	7.49×10^{-4}
3000	99.90	1.05×10^{-3}

Figure 6. Calculated branching ratios vs $1000/T$ between 200 and 3000 K for reaction CF$_3$CH(OH)CF$_3$ + OH.

where a is the total instantaneous infrared radiative forcing (W m^{-2} ppbv^{-1}), AGWP is the absolute global warming potential for the reference compound, and $F(\nu_k)$ is the radiative forcing function per unit cross section per wavenumber[40] (W m^{-2}(cm^{-1})$^{-1}$)(cm^2 molecule^{-1})$^{-1}$) evaluated at the scaled band center frequency (ν_k). The GWPs computed for different time horizons and the lifetimes are tabulated in Table 6. The GWPs are found to be reasonably larger for this compound.

In conclusion, though the atmospheric lifetimes of test molecule (CF$_3$CH(OH)CF$_3$) is long, when compared with CFCs, it can be considered as short-lived species. GWPs are also relatively smaller, when compared with those of CFCs (e.g., GWP of CFC-11 is 6330 for a 20-year time horizon) and HFCs.

4.3. OH Initiated Oxidation. OH initiated atmospheric degradation of CF$_3$CH(OH)CF$_3$ is similar to isopropanol.[41] The mechanism for the oxidation of CF$_3$CH(OH)CF$_3$ in a nitrogen-rich environment is shown in Figure 7. The reaction of CF$_3$CH(OH)CF$_3$ with OH will go through mainly via H-abstraction from methyne (−CH−) group, and it leads to the formation of the CF$_3$C(OH)CF$_3$ radical. Then the CF$_3$C(OH)CF$_3$ radical react with O$_2$ mainly leads to the formation of hexafluoroacetone through H-atom abstraction, and also it can form a fluorosubstituted peroxy radical (CF$_3$C(OH)(OO)CF$_3$) as a minor product. If this peroxy radical is more stable, it leads to the formation of acetic acid through reaction with NO. When compared with hexafluoroisopropanol (CF$_3$CH(OH)CF$_3$), hexafluoroacetone (CF$_3$C(O)CF$_3$) is less reactive. So, the removal of CF$_3$C(O)CF$_3$ from the atmosphere is slower. The resulting radicals form hexafluoroperoxyacetyl nitrate, in the presence of NO$_x$, which may further act as a resource for ozone formation in the troposphere.

Table 6. Atmospheric Lifetimes of Hexafluoroisopropanol (CF$_3$CH(OH)CF$_3$) and Its GWPs Computed at 272 K Using the M06-2X/6-31+G(d,p) Level of Theory

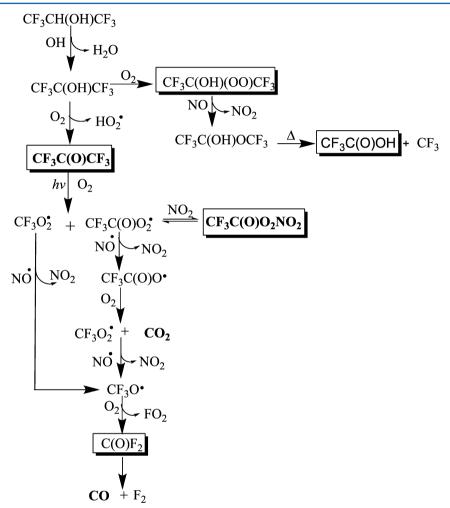| | atmospheric lifetime, years | | GWPs at time horizons | | | | | |
| | | | present study (years) | | | reported[3] (years) | | |
molecule	present study	reported	20	100	500	20	100	500
CF$_3$CH(OH)CF$_3$	1.21	1.94[3]	304.2	93.1	29.07	830	240	72

Figure 7. OH initiated atmospheric degradation mechanism for CF$_3$CH(OH)CF$_3$ in the NO-rich environment. Compounds in the boxes are stable products.

CONCLUSIONS

In the present work, the kinetics of hydrogen abstraction from CF$_3$CH(OH)CF$_3$ by OH radical was investigated at M06-2X/6-31+G(d,p) theory. The M06-2X functional given reasonably close results to that of experimental data available on CF$_3$CH(OH)CF$_3$ + OH reaction. Two classes of H-abstraction reaction channels are identified. The theoretical rate coefficients for each reaction channel are calculated by canonical variation transition state theory (CVT) with the small-curvature tunneling correction (SCT) at the M062X theory. The results are consistent with the reported experimental values in the corresponding measured temperature regions. We have noticed that, for this title reaction, hydrogen abstraction from the −CH− group is the main reaction channel. This compound's atmospheric lifetime seems to be larger and so are the GWPs. The OH initiated atmospheric degradation mechanism of CF$_3$CH(OH)CF$_3$ in the NO rich environment is discussed.

ASSOCIATED CONTENT

S **Supporting Information**
Structural parameters and vibrational frequencies of all the optimized geometries at both M06-2X and MPW1K level of theories. This material is available free of charge via the Internet at http://pubs.acs.org.

AUTHOR INFORMATION

Corresponding Author
*E-mail: rajakumar@iitm.ac.in.
Notes
The authors declare no competing financial interest.

ACKNOWLEDGMENTS

■ REFERENCES

(1) Global Ozone Research and Monitoring Project - Report No. 52 Scientific Assessment of Ozone Depletion; World Meteorological Organization: Geneva, 2010; p 516.

(2) Hayman, G. D.; Derwent, R. G. Atmospheric Chemical Reactivity and Ozone-Forming Potentials of Potential CFC Replacements. *Environ. Sci. Technol.* **1997**, *31*, 327−336.

(3) Orkin, V. L.; Khamaganov, V. G.; Kurylo, M. J. High Accuracy Measurements of OH Reaction Rate Constants and IR Absorption Spectra: Substituted 2-Propanols. *J. Phys. Chem. A* **2012**, *116*, 6188−6198.

(4) Tokuhashi, K.; Nagai, H.; Takahashi, A.; Kaise, M.; Kondo, S.; Sekiya, A.; Takahashi, M.; Gotoh, Y.; Suga, A. Measurement of the OH Reaction Rate Constants for CF_3CH_2OH, $CF_3CF_2CH_2OH$, and $CF_3CH(OH)CF_3$. *J. Phys. Chem. A* **1999**, *103*, 2664−2672.

(5) Gonzalez-Lafont, A.; Truong, T. N.; Truhlar, D. G. Interpolated variational transition-state theory: Practical methods for estimating variational transition-state properties and tunneling contributions to chemical reaction rates from electronic structure calculations. *J. Chem. Phys.* **1991**, *95*, 8875−8894.

(6) Garrett, B. C.; Truhlar, D. G. Generalized transition state theory. Classical mechanical theory and applications to collinear reactions of hydrogen molecules. *J. Phys. Chem.* **1979**, *83*, 1052−1079.

(7) Garrett, B. C.; Truhlar, D. G.; Grev, R. S.; Magnuson, A. W. Improved treatment of threshold contributions in variational transition-state theory. *J. Phys. Chem.* **1980**, *84*, 1730−1748.

(8) Lu, D. H.; Truong, T. N.; Melissas, V. S.; Lynch, G. C.; Liu, Y. P.; Garrett, B. C.; Steckler, R.; Isaacson, A. D.; Rai, S. N.; Hancock, G. C. POLYRATE 4: A new version of a computer program for the calculation of chemical reaction rates for polyatomics. *Comput. Phys. Commun.* **1992**, *71*, 235−262.

(9) Liu, Y. P.; Lynch, G. C.; Truong, T. N.; Lu, D. H.; Truhlar, D. G.; Garrett, B. C. Molecular modeling of the kinetic isotope effect for the [1,5]-sigmatropic rearrangement of cis-1,3-pentadiene. *J. Am. Chem. Soc.* **1993**, *115*, 2408−2415.

(10) Zhao, Y.; Truhlar, D. G. The M06 suite of density functionals for main group thermochemistry, thermochemical kinetics, non-covalent interactions, excited states, and transition elements: two new functionals and systematic testing of four M06-class functionals and 12 other functionals. *Theor. Chem. Acc.* **2008**, *120*, 215−241.

(11) Zhao, Y.; Truhlar, D. G. Density Functionals with Broad Applicability in Chemistry. *Acc. Chem. Res.* **2008**, *41*, 157−161.

(12) Lynch, B. J.; Fast, P. L.; Harris, M.; Truhlar, D. G. Adiabatic Connection for Kinetics. *J. Phys. Chem. A* **2000**, *104*, 4811−4815.

(13) Zhao, Y.; Truhlar, D. G. Hybrid Meta Density Functional Theory Methods for Thermochemistry, Thermochemical Kinetics, and Noncovalent Interactions: The MPW1B95 and MPWB1K Models and Comparative Assessments for Hydrogen Bonding and van der Waals Interactions. *J. Phys. Chem. A* **2004**, *108*, 6908−6918.

(14) Balaganesh, M.; Rajakumar, B. Rate Coefficients and Reaction Mechanism for the Reaction of OH Radicals with (E)-$CF_3CH=CHF$, (Z)-$CF_3CH=CHF$, (E)-$CF_3CF=CHF$, and(Z)-$CF_3CF=CHF$ between 200 and 400 K: Hybrid Density Functional Theory and Canonical Variational Transition State Theory Calculations. *J. Phys. Chem. A* **2012**, *116*, 9832−9842.

(15) Jissy, A. K.; Ashik, U. P. M.; Datta, A. Nucleic Acid G-quartets: Insights into Diverse Patterns and Optical Properties. *J. Phys. Chem. C* **2011**, *115*, 12530−12546.

(16) Nijamudheen, A.; Jose, D.; Shine, A.; Datta, A. Molecular Balances Based on Aliphatic CH−π and Lone-Pair−π Interactions. *J. Phys. Chem. Lett.* **2012**, *3*, 1493−1496.

(17) Jissy, A. K.; Datta, A. Effect of External Electric Field on H-Bonding and p-Stacking Interactions in Guanine Aggregates. *ChemPhysChem* **2012**, *13*, 4163−4172.

(18) Abraham, S. A.; Jose, D.; Datta, A. Do Cation⋯p Interactions Always Need to be 1:1? *ChemPhysChem* **2012**, *13*, 695−698.

(19) Truhlar, D. G.; Kupperman, A. Exact tunneling calculations. *J. Am. Chem. Soc.* **1971**, *93*, 1840−1851.

(20) Gonzalez, C.; Schlegel, H. B. An improved algorithm for reaction path following. *J. Chem. Phys.* **1989**, *90*, 2154−2161.

(21) Frisch, M. J.; Trucks, G. W.; Schlegel, H. B.; Scuseria, G. E.; Robb, M. A.; Cheeseman, J. R.; Scalmani, G.; Barone, V.; Mennucci, B.; Petersson, G. A.; et al. *Gaussian 09*, Revision B.01; Gaussian, Inc.: Wallingford, CT, 2010.

(22) Dennington, I. I. R.; Keith, T.; Millam, J.; Eppinnett, K.; Hovell, W. L.; Gilliland, R. *GaussView*, Version 3.09; Semichem, Inc.: Shawnee Mission, KS, 2003.

(23) Zheng, J.; Zhang, S.; Lynch, B. J.; Corchado, J. C.; Chuang, Y.-Y.; Fast, P. L.; Hu, W.-P.; Liu, Y.-P.; Lynch, G. C.; Nguyen, K. A.; et al. *POLYRATE*, version 2008; University of Minnesota: Minneapolis, MN, 2009.

(24) Zheng, J.; Zhang, S.; Corchado, J. C.; Chuang, Y.-Y.; Coitiño, E. L.; Ellingson, B. A.; Truhlar, D. G. *GAUSSRATE*, version 2009-A; University of Minnesota: Minneapolis, MN, 2010.

(25) Chase, M. W. NIST-JANAF Thermo chemical Tables. *J. Phys. Chem. Ref. Data, Monograph* **1998**, *9*, 1.

(26) Lide, D. R. *CRC Handbook of Chemistry and Physics*, 80th ed.; CRC Press: New York, 1999.

(27) Boys, S. F.; Bernardi, F. The calculation of small molecular interactions by the differences of separate total energies. Some procedures with reduced errors. *Mol. Phys.* **1970**, *19*, 553−566.

(28) Wang, Y.; Liu, J.-y.; Li, Z.-s.; Wang, L.; Wu, J.-y.; Sun, C.-c. Direct Dynamics Study on Hydrogen Abstraction Reaction of $CF_3CF_2CH_2OH$ with OH Radical. *J. Phys. Chem. A* **2006**, *110*, 5853−5859.

(29) Liu, J.; Li, Z.; Dai, Z.; Huang, X.; Sun, C. Direct ab Initio Dynamics Study on the Hydrogen Abstraction Reaction of CH_3CCl_3 + OH → CH_2CCl_3 + H_2O. *J. Phys. Chem. A* **2003**, *107*, 6231−6235.

(30) Sheng, L.; Li, Z.; Liu, J.; Xiao, J.; Sun, C. Ab Initio Direct Dynamics Studies on the Reactions of H Atoms with CCl_4 and $CHCl_3$. *J. Phys. Chem. A* **2002**, *106*, 12292−12298.

(31) Zhang, Q.; Wang, S.; Gu, Y. Direct ab Initio Dynamics Studies of the Reactions of H with $SiH4-nCl_n$ (n = 1−3). *J. Phys. Chem. A* **2002**, *106*, 3796−3803.

(32) Zhang, Q.; Zhang, R.; Gu, Y. Kinetics and Mechanism of O (^{3}P) Reaction with CH_3CHF_2: A Theoretical Study. *J. Phys. Chem. A* **2004**, *108*, 1064−1068.

(33) Luo, Q.; Li, Q. S. Direct ab Initio Dynamics Study of the Unimolecular Reaction of CH_2FO. *J. Phys. Chem. A* **2004**, *108*, 5050−5056.

(34) Dash, M. R.; Rajakumar, B. Abstraction Kinetics of H-Atom by OH Radical from Pinonaldehyde ($C_{10}H_{16}O_2$): Ab Initio and Transition-State Theory Calculations. *J. Phys. Chem. A* **2012**, *116*, 5856−5866.

(35) Blowers, P.; Moline, D. M.; Tetrault, K. F.; Wheeler, R. R.; Tuchawena, S. L. Prediction of Radiative Forcing Values for Hydrofluoroethers Using Density Functional Theory Methods. *J. Geophys. Res. Atmos.* **2007**, *112*, D15108.

(36) Blowers, P.; Moline, D. M.; Tetrault, K. F.; Wheeler, R. R.; Tuchawena, S. L. Global Warming Potentials of Hydrofluoroethers. *J. Geophys. Environ. Sci. Technol.* **2008**, *42*, 1301−1307.

(37) *Radiative forcing of climate change and an evaluation of the IPCC IS92 Emission Scenarios*; Houghton, J. T., Filho, L. G. M., Bruce, B., Lee, H., Callander, B. A., Haites, E., Harris, N., Maskell, K., Eds.; Intergovernmental Panel on Climate Change (IPCC), climate change, 1994; Cambridge University Press: New York, 1995.

(38) *Climate Change, The IPCC Scientific assessment*; Houghton, J. T., Jenkins, G. J., Ephraums, J. J., Eds.; Cambridge University Press: New York, 1990.

(39) Alecu, I. M.; Zheng, J.; Zhao, Y.; Truhlar, D. G. Computational Thermochemistry: Scale Factor Databases and Scale Factors for Vibrational Frequencies Obtained from Electronic Model Chemistries. *J. Chem. Theory Comput.* **2010**, *6*, 2872−2887.

(40) Pinnock, S.; Hurley, M. D.; Shine, K. P.; Wallington, T. J.; Smyth, T. J. Radiative forcing of climate by hydrochlorofluorocarbons and hydrofluorocorbons. *J. Geophys. Res. Atmos.* **1995**, *100*, 23227−23238.

(41) Rajakumar, B.; McCabe, D. C.; Talukdar, R. K.; Ravishankara, A. R. Rate Coefficients for the Reactions of OH with n-Propanol and iso-Propanol between 237 and 376 K. *Int. J. Chem. Kinet.* **2010**, *42*, 10−24.

4544

dx.doi.org/10.1021/jp4006907 | *J. Phys. Chem. A* 2013, 117, 4534−4544